Original Research

Ab initio Studies of the Structural, Electronic and Mechanical Properties of $Zn_{1-x}Cr_xTe$

A. A. Audu[a,*], W. A. Yahya[a], A. A. Abdulkareem[a]

[a]Department of Physics and Materials Science, Kwara State University, Malete, Kwara State, Nigeria

Abstract

The structural, electronic, and mechanical properties of $Zn_{1-x}Cr_xTe$ alloys (for x = 0, 0.25, and 1) have been investigated using *ab initio* plane-wave ultrasoft pseudopotential calculations based on the density functional theory (DFT). The calculations have been carried out within the local density approximation (LDA), generalized gradient approximation (GGA), and Meta-GGA (T-B09) exchange-correlation functionals as implemented in the Quantum Espresso suite of codes and Elk Full-Potential Linearized Augmented Plane-wave (FP-LAPW) codes. As it is well known that LDA and GGA underestimate experimental band gaps, we made attempts to improve on the calculated band gaps using Gaussian-Perdew-Burke-Ernzerhof (Gau-PBE), hybrid functionals, and TB09. We found that the use of TB09 gives the best estimation for the electronic band gap within $\approx 1\%$ error. The calculated lattice constants are all in good agreement with the experimental results. The p-type doped ZnTe with chromium (Cr) atom was also investigated (50% Cr impurity added). The Zinc-blende (ZB) CrTe shows a magnetic property, and electronic structure calculations suggest that it may have applications in spintronics. A $1 \times 2 \times 2$ super-cell (25% Cr impurity added) was created to further study the effects of impurities on the electronic and mechanical properties of ZB ZnTe. The results show changes in the lattice parameters, electronic properties, and mechanical properties. The three materials satisfy the mechanical stability conditions, which suggests that they are all mechanically stable. They are also anisotropic. Moreover, ZnTe and Zn_3CrTe_4 are ductile while CrTe is brittle.

Keywords: Plane-wave Ultrasoft Pseudopotential, Density Functional Theory (DFT), Electronic Properties, Mechanical Properties, ZnTe

1. Introduction

In the last few decades, researchers have extensively investigated the structural and electronic properties of II-VI semiconductors because of their applications in the development of new electronic and optoelectronic devices [1], [2].

---

*Corresponding author tel. no: +2347060540025
Email address: auduayinde@gmail.com (A. A. Audu)

The study of these II-VI semiconductors such as the mono-chalcogenide Zinc e.g. ZnTe, ZnS, and ZnSe has been used in many technological applications such as optical memories of high density, semiconductor laser devices, blue light emitted diodes (LEDs), laser diodes, components of microwave generators, transparent photodetectors conductors, development of new nanotechnologies e.t.c [3], [1]. It can also be used in solar cells, as photovoltaic devices, remote control systems, thin films, transistors, Terahertz emitter, detector, and imaging systems [4].

The knowledge of the structural and electronic properties of these materials e.g Zinc Telluride (ZnTe) can play a crucial role in the understanding of their fundamental solid-state phenomenon, their optical and transport properties [1], [5]. The lattice constant and the bulk moduli could help to determine the hardness of a material [6]. The theoretical studies of the electronic bandstructure of ZnTe using LDA and GGA exchange-correlation functional has resulted into the underestimation of the bandstructure [2]. There is the need to on the theoretical calculations of the electronic band gap of ZnTe using new pseudopotentials (with different exchange-correlation functionals) and full-potential calculations with Meta-GGA exchange-correlation functionals.

In this work, the structural, electronic, and mechanical properties of Zinc-blende ZnTe has been investigated using the ultrasoft pseudo-potential and full-potential linearised augumented plane wave [7] approaches based on density functional theory (DFT) [8]. The paper is organised as follows. In Section [2], the computational details are presented. This is followed by the results of the structural, electronic, and mechanical properties of pure and Cr-doped ZnTe in Section [3]. The conclusion is given in Section [4].

2. Computational Details

The calculations have been carried out using ultrasoft pseudo-potential [9] and full potential linearized plane wave (FP-LAPW) method [7] in the framework of the density functional theory (DFT) [8], as implemented in the Quantum ESPRESSO (QE) and Elk codes [10]. The Kohn-Sham equations [11-12] was solved self-consistently. The computations have been caried out using LDA, GGA (PBE [13] and PBEsol [14], Gau- PBE, hybrid, and META-GGA exchange correlation functionals [15-16]. Geometrical optimisation was carried out and energy convergence was ensured. A kinetic energy cut-off of 70 Ry and charge density cut-off of 700 Ry for the plane wave basis set has been employed. A Monkhorst-Pack grid of 10×10×10 k-point mesh for the Brillouin-zone integrations [17] was used. The ground state properties of $Zn_{1-x}Cr_xTe$ for x = 0, 0.25, and 1 have been obtained for each structure using the Birch-Murnaghan equation of state (EOS) [18] by fitting the total energy with the unit cell volume. A $1 \times 2 \times 2$ supercell was created to obtain Zn_3CrTe_4 when 25% Cr impurities was added at one of the Zn sites. The stability conditions of the cubic ZnTe are tested using the equations:

$$C_{11} - C_{12} > 0, \tag{1}$$

$$C_{44} > 0, \tag{2}$$

$$C_{11} + 2C_{12} > 0, \tag{3}$$

$$C_{12} < B < C_{11}. \tag{4}$$

The bulk modulus (B), shear modulus (G), Young's modulus (E), and the Poisson's ratio (n) are computed using:

$$B = \frac{C_{11} + 2C_{12}}{3}, \tag{5}$$

$$G = \frac{C_{11} - C_{12} + 3C_{44}}{5}, \tag{6}$$

$$E = \frac{9GB}{(3B + G)}, \tag{7}$$

and

$$n = \frac{1}{2}\left[\frac{B - (\frac{2}{3})G}{B + (\frac{1}{3})G}\right], \tag{8}$$

respectively. The anisotropy factor A (shows the variation of elastic properties with direction), internal strain parameters (ξ), and the Debye temperature (θ_D) are also computed via

$$A = \frac{2C_{44}}{C_{11} - C_{12}}, \tag{9}$$

$$\xi = \frac{C_{11} + 8C_{12}}{7C_{11} + 2C_{12}}, \tag{10}$$

respectively. Debye temperature (θ_D) is one of the fundamental parameters related to many physical properties of materials such as specific heat and melting temperature. The Debye temoerature (θ_D) is deduced by using the following equation:

$$\theta_D = \frac{\hbar}{k} \left[\frac{3n}{4\pi} \left(\frac{N_A \rho}{M} \right) \right]^{\frac{1}{3}} V_D, \tag{11}$$

where V_D is given as

$$V_D = \left[\frac{1}{3} \left(\frac{1}{V_L^3} + \frac{2}{V_T^3} \right) \right]^{\frac{-1}{3}}. \tag{12}$$

For the orthorhombic structure Zn_3CrTe_4 (i.e. when x = 0.25), the mechanical stability and anisotropic factor are determined via:

$$C_{11}, C_{22}, C_{33}, C_{44}, C_{55}, C_{66} > 0, \tag{13}$$

$$C_{11} + C_{22} - 2C_{12} > 0, \tag{14}$$

$$C_{11} + C_{33} - 2C_{13} > 0, \tag{15}$$

$$C_{22} + C_{33} - 2C_{23} > 0, \tag{16}$$

$$C_{11} + C_{22} + C_{33} + 2(C_{12} + C_{13} + C_{23}) > 0. \tag{17}$$

The shear anisotropic factors are among the used criteria to measure the degree of anisotropy in the bonding between atoms in different planes. For the {100} shear planes between the <011> and <010> directions in orthorhombic crystals, the anisotropy [19].

$$A_1 = \frac{4C_{44}}{C_{11} + C_{33} - 2C_{13}}, \tag{18}$$

for the {010} shear planes between <101> and <001> directions the anisotropy

$$A_2 = \frac{4C_{55}}{C_{22} + C_{33} - 2C_{23}}, and \tag{19}$$

and for the {001} shear planes between <110> and <010> directions the anisotropy

$$A_3 = \frac{4C_{66}}{C_{11} + C_{22} - 2C_{12}}. \tag{20}$$

3. Results and Discussion

3.1. Structural properties

The geometry optimization for each of the three exchange-correlation (XC) functionals have been carried out to obtain the equilibrium lattice constants. These are obtained using the third-order Birch-Murnaghan equation of state (EOS) given by [18]

$$E(V) = E_0 + \frac{9}{16} V_0 B \left\{ \left[\left(\frac{V}{V_0} \right)^{\frac{2}{3}} - 1 \right]^3 B' + \left[\left(\frac{V}{V_0} \right)^{\frac{2}{3}} - 1 \right]^2 \left[6 - 4 \left(\frac{V}{V_0} \right)^{\frac{2}{3}} \right] \right\} \tag{21}$$

Table 1. The calculated optimized results for the lattice constants (a), b(Å), and c(Å), unit cell volume (V_0), the bulk modulus (B), and its derivative (B') of ZnTe, CrTe, and Zn_3CrTe_4 using LDA, GGA (PBE), and GGA (PBEsol) XC functionals

	a(Å)	b(Å)	c(Å)	V_0(Å^3)	$B(GPa)$	B'
LDA(ZnTe)	6.104	-	-	56.86	52.90	4.70
PBE(ZnTe)	6.099	-	-	56.73	45.20	4.63
PBEsol(ZnTe)	6.104	-	-	56.84	49.80	4.68
PBEsol(CrTe)	6.160	-	-	58.48	50.90	4.608
PBEsol(Zn_3CrTe_4)	21.35	0.709	0.354	180.78	64.35	5.51
Experiment (ZnTe)	6.101 [20]	-	-	56.82 [21], 56.91 [22]	50.50 [21]	5.00 [23]
Theory (ZnTe)	6.063 [24]	-	-	56.07 [25], 55.21 [22]	55.21 [22]	4.7 [21]

and

$$P = \frac{3}{2}B\left[\left(\frac{V}{V_0}\right)^{-\frac{7}{3}} - \left(\frac{V}{V_0}\right)^{-\frac{5}{3}}\right] \times \left\{1 + \frac{3}{4}(B'-4)\left[\left(\frac{V}{V_0}\right)^{-\frac{2}{3}} - 1\right]\right\}, \tag{22}$$

where $E(V)$ is the DFT ground-state energy with the cell volume, V. V_0 is the unit cell volume at zero pressure, (B) denotes the bulk modulus, the bulk modulus pressure derivative (B') is expressed as (B') = $\frac{\partial B}{\partial P}$ at $P = 0$. These EOS parameters computed for the different exchange correlation functionals are listed in Table 1. The Table shows that the lattice parameters for ZnTe and CrTe agree with the experimental value and other theoretical calculations. The PBEsol functional gives the most accurate values of the lattice parameters and bulk modulus of ZnTe, when compared with experimental data. Figure 1 shows the plot of the energy versus volume for the cubic ZnTe. The data in the Figure were used to obtain the minimum lattice parameter..
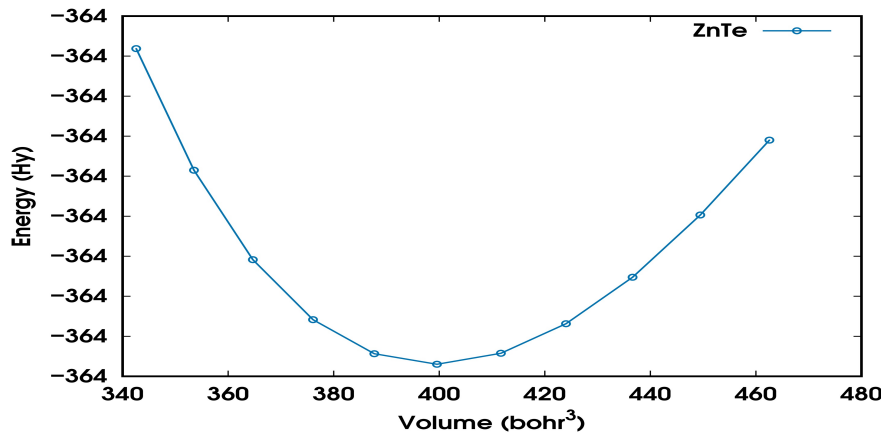

Figure 1. Energy-volume curve of ZnTe using LDA XC functional

3.2. Electronic Properties

The electronic band structure for ZnTe (a face centered cubic crystal) for the three different types of XC functionals has been calculated using ultrasoft pseudopotentials along the selected high symmetry k path Γ-X-W-K-Γ-L-U-W-L-K-U-X within the first Brillouin zone of its primitive cell. Figure 2 shows the band structure of ZnTe using both PBEsol and TB09. The left panel shows the band structure using PBEsol while the panel on the right shows the band structure using TB09. The PBEsol XC functional with a 1.23 eV energy band gap, highly underestimates the experimental band gap of 2.38 eV. It is a known fact that LDA and GGA underestimate band gaps [26], [27]. This

Table 2. Comparison of the calculated results of the estimated band gaps (E_g) in eV by different exchange-correlation functionals

	Band gap (eV)	Other calculations
LDA	1.27	1.33 [28]
GGA(PBE)	1.07	1.04 [2]
GGA(PBEsol)	1.23	
Gau-PBE	1.62	
HSE	1.84	2.19 [2]
TB09	2.35	
Experiment	2.38 [27]	

has been atrributed to the inability of the LDA and GGA functionals to access the excited states. This is inherent for non interacting one-electron Kohn-Sham (KS) scheme. Another reason for the underestimation of the experimental band gap by the LDA and GGA XC functionals is the partial removal of self-interaction in the DFT [26]. The TB09 gives a wider and more accurate band gap compared with the PBEsol.

The calculated energy band gaps for all the XC functionals are shown in Table 2. We observe from the Table that although GAU-PBE and HSE give better descriptions of the band gaps than LDA and GGA functionals, the TB09 gives the best result with a value of 2.35 eV compared to the experimental value of 2.38.
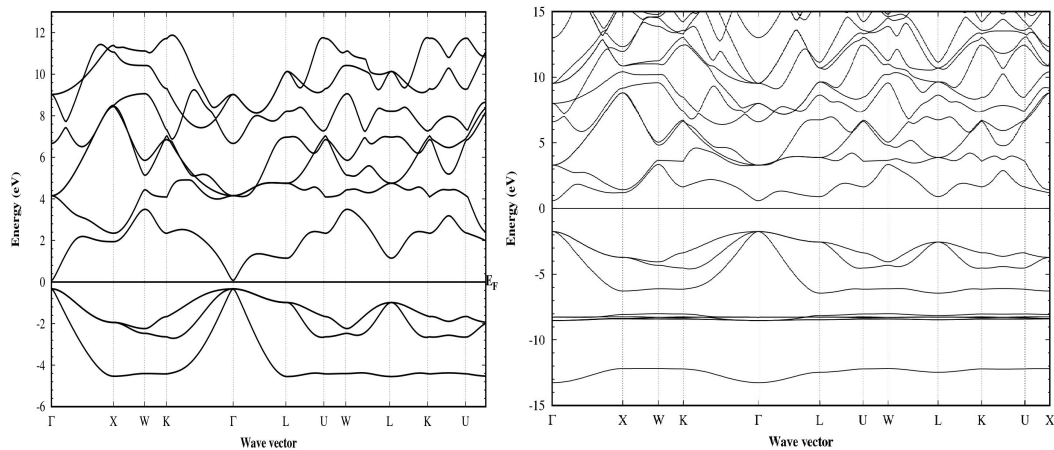

Figure 2. Band structure of ZnTe using PBEsol (left) and TB09 (right) along high symmetry points in the Brillouin zone

In order to study the electronic properties of CrTe and Zn_3CrTe_4, spin-polarised calculations were carried out. Spin-polarised calculations are required for the two materials because, as shown in Figure 3, calculations involving spin-polarisation (Magnetic) give lower energy compared to calculations without spin-polarisation (Non-magnetic). This suggests that the materials have magnetic properties. Moreover the calculated magnetization for CrTe is 4 bohr mag/cell, with a magnetic moment of 3.45 μ_B. Figure 3 shows only the results for CrTe. The same thing applies to Zn_3CrTe_4. The fact that the two materials have non-zero magnetic moments indicates that they have magnetic properties.
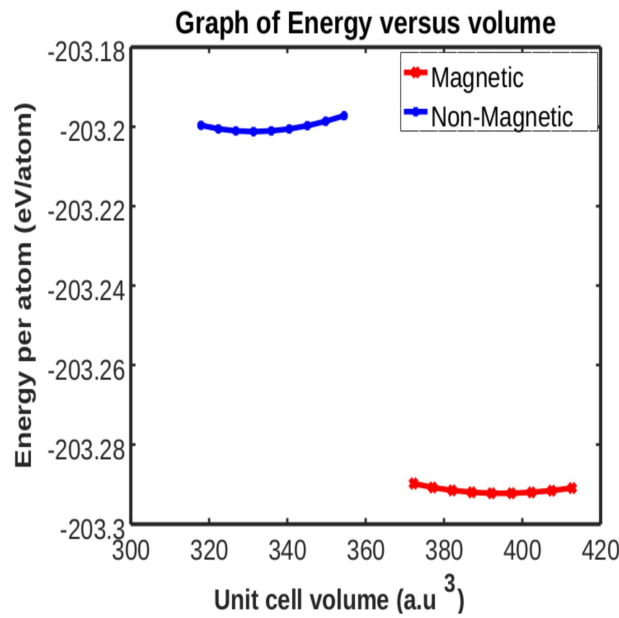
Figure 3. Variation of energy versus volume for calculation involving spin-polarisation (Magnetic) and without spin polarisation (Non-magnetic)
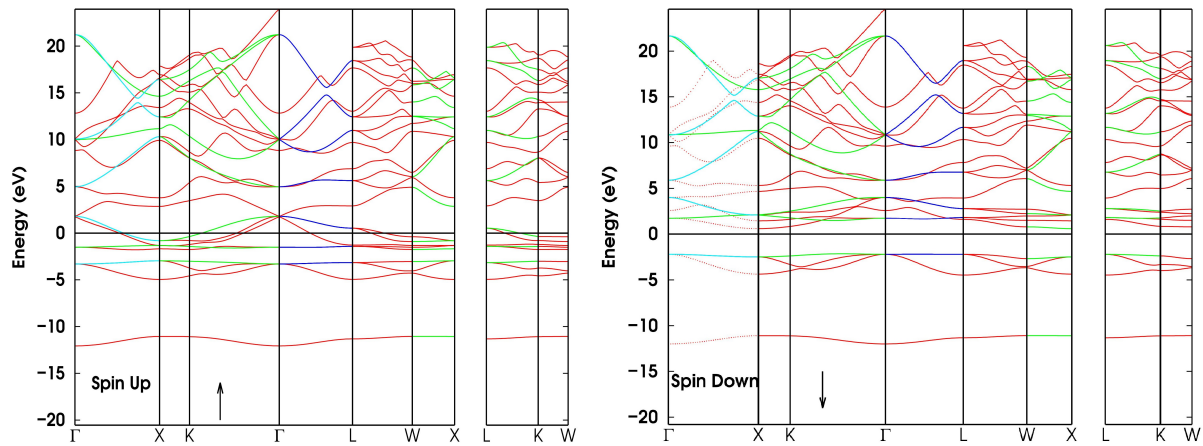

Figure 4. Electronic band structures of CrTe showing spin up and spin down

The higher values of Young's modulus in comparison to the bulk modulus as shown in Table 3 shows that ZnTe is hard to break [6]. A high $\frac{B}{G}$ value is associated with ductility and low $\frac{B}{G}$ value is associated with brittleness. The critical value which separates ductile and brittle materials is about 1.75 [19]. The calculated values of 2.03 and 1.99 using LDA and PBEsol XC functionals predicts ductility in ZnTe materials as shown in Table 2. Stability of materials (crystals) against shear deformation can be quantified using Poisons's ratio (*n*). It usually ranges from −1 to 0.5. It also provides more information about the characteristics of the bonding forces (nature of bond) than any of the elastic constants (C_{ij}). For central force solids, the lower and upper limits are 0.25 and 0.5 [32]. The value of Poisson ratio is of the order of 0.1 when it comes to covalent bonded materials while for ionic compounds, the value of Poisson ratio is usually 0.25 [1]. The values of Poisson ratio, *n*, (0.283, 0.257, and 0.272) for *ZnTe*, *CrTe*, and Zn_3CrTe_4, respectively, show that the interatomic forces are central forces and are of ionic bondings. The ionic contribution is
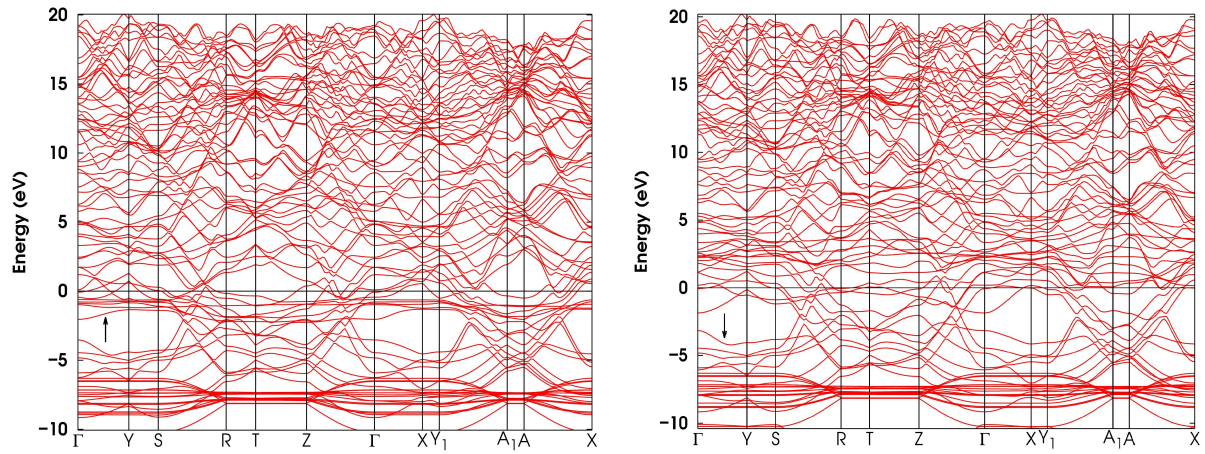
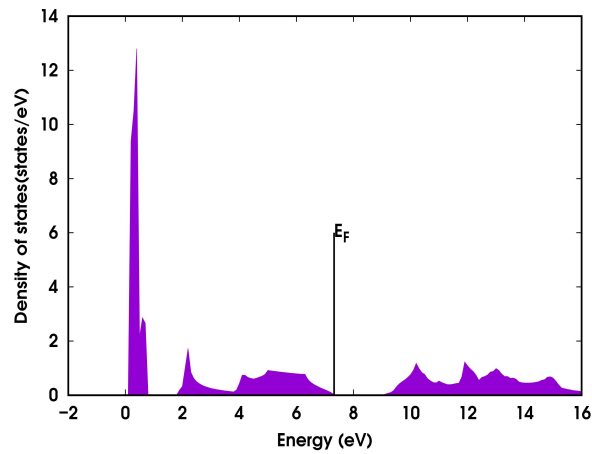Figure 5. Electronic band structures of Zn_3CrTe_4 showing spin up and spin down

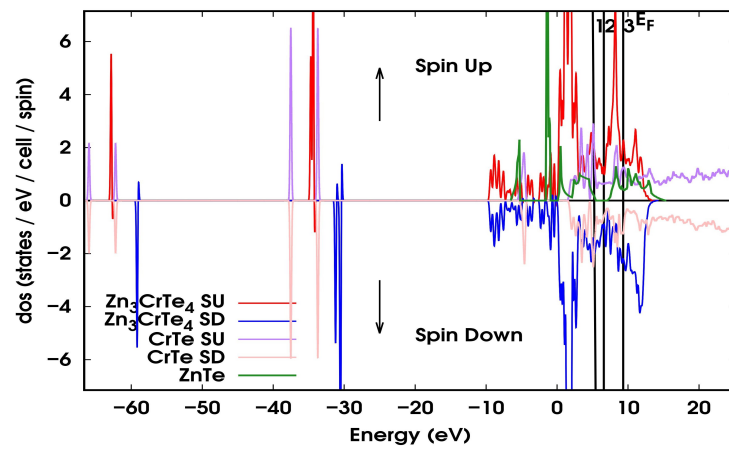Figure 6. Total density of states of ZnTe using PBE exchange-correlation functional

Figure 7. Total density of states of ZnTe, CrTe, and Zn_3CrTe_4 showing spin up and spin down

Table 3. The calculated results for the elastic constants C_{ij} (all in GPa); C_{11}, C_{12}, C_{44}, elastic modulus (all in GPa), bulk modulus B, shear modulus G, Young's modulus E, Poisson's ratio (n), Anisotropy index (A), and internal strain parameter (ξ) of ZB ZnTe

Elastic parameters	LDA	GGA (PBE)	GGA (PBEsol)	Exp.	Other theory
C_{11}	78.29	62.33	72.45	71.70 [29]	64.70 [30], 82.00 [7]
C_{12}	44.61	32.09	41.06	40.70 [29]	36.00 [30], 42.00 [7]
C_{44}	38.28	33.86	36.16	31.20 [29]	40.1 [30], 50.54 [24]
B	55.84	42.17	51.53	50.5 [21]	45.60 [30]
G	27.53	24.50	25.87	29.50 [31]	26.60 [30]
$\frac{B}{G}$	2.03	1.72	1.99		
E	70.89	61.53	66.43	75.00 [31]	66.70 [30]
n	0.287	0.256	0.283		0.256 [30]
A	2.27	2.24	2.30		3.86 [1]
ξ	0.683	0.637	0.680		0.743 [1]

Table 4. The calculated results for the elastic constants C_{ij} (all in GPa), bulk modulus (B), shear modulus (G), Young's modulus (E), Poisson's ratio (n), and Anisotropy index (A), and internal strain parameter (ξ) of Zn_3CrTe_4. using PBEsol XC functional

	C_{11}	C_{12}	C_{13}	C_{22}	C_{23}	C_{33}	C_{44}	C_{55}	C_{66}
ZnTe	72.45	41.06	36.16						
CrTe	53.91	51.30	36.61						
Zn_3CrTe_4	133.82	114.77	117.56	49.49	31.03	29.92	33.97	36.02	56.70

	B	G	$\frac{B}{G}$	E	n	A_1	A_2	A_3	A	ξ
ZnTe	51.53	25.87	1.99	66.43	0.283				2.30	0.683
CrTe	52.17	30.22	1.73	75.98	0.257				37.923	0.967
Zn_3CrTe_4	68.82	36.95	1.863	94.01	0.272	2.04	1.29	0.91		

also dominant in these compounds which makes them useful for high electro-optical and electromechanical coupling [32]. The value of Poison's ratio can also be used to investigate the flexibility materials. The larger value of Poison's ratio signifies the plasticity in materials [32].

The computed anisotropy (A) for ZnTe and CrTe are 2.30 and 37.923, respectively. Since $A > 0$, the two materials have elastic anisotropy properties. Similarly, since A_1, A_2, and A_3 are greater than zero, Zn_3CrTe_4 also has elastic anisotropy property. Anisotropy has an important implication in engineering and science, since it is highly correlated with the possibility to induce microcracks in materials. Elastic anisotropy is an important physical property of materials and plays vital roles in technological and industrial applications [1].

4. Conclusion

The density functional theory calculations of structural, electronic, and mechanical properties of pure and Cr doped zinc telluride (ZnTe) has been presented. The calculations were carried out within the LDA, GGA (PBE and PBEsol), hybrid functionals, and Meta-GGA exchange-correlation functionals using *ab initio* plane-wave ultrasoft pseudopotential and full-potential linearised augmented-plane-wave. The Meta-GGA (TB09) was employed to improve the theoretical band gap calculation of PBE and PBEsol. An energy band gap of 2.35 eV was obtained using the TB09 which shows an excellent agreement with the experimental value of 2.38 eV with $\approx$ 1% error. PBEsol exchange correlation functional predicts the best estimation of the bulk modulus (B) with 1.4% error. The structural and electronic properties calculations show that CrTe and Zn_3CrTe_4 have magnetic properties. CrTe has a magnetic moment of 3.45 μ_B. The band structure plots also show that CrTe can be used in spintronics applications, and that Zn_3CrTe_4 is a magnetic metal. The elastic constants, bulk modulus, shear modulus, Young's modulus, Poisson's ratio, and Debye temperature were also computed. The three materials satisfy the mechanical stability conditions, which suggests that they are all mechanically stable. They are also anisotropic. Moreover, ZnTe and Zn_3CrTe_4 are ductile while CrTe is brittle.

References

[1] M. Bilal, M. Shafiq, I. Ahmad & I. Khan, "First principle studies of structural, elastic, electronic and optical properties of zn-chalcogenides under pressure", *Journal of Semiconductors*, **35**: (2014) 07200.

[2] P. Gopal, M. Fornari & M. Nardelli, "Improved predictions of the physical properties of zn and cd-based wide band-gap semiconductors: A validation of the acbno functional", *Physical Review B*, **91**: (2015) 245202.

[3] A. Rachidi, E. H. Atmani, N. Fazouan & M. Boujnah, "A study by ab-initio calculation of structural and electronic properties of semiconductor nanostructures based on ZnSe", *Materials Sciences and Applications*, **7**: (2016) 562–573.

[4] S. Ferahtia, S. Saib & N. Bouarissa, "Thermodynamic properties of ZnTe in zinc-blende and wurtzite phases", *International Journal of Modern Physics B*, **30**: (2016).

[5] K. Imad & A. Iftikhar, "Theoretical studies of the band structure and optoelectronic properties of ZnO_xS_{1-X}", *International Journal of Quantum Chemistry*, **133(9)**: (2013) 1285.

[6] P. F. Yuan & Z. J. Ding, "Ab initio calculation of elastic properties of rock-salt and zinc-blende MgS under pressure", *Physical Review B*, **403(12)** (2008).

[7] R. Khenata, A. Bouhemadou, & M. Sahnoun, "Electronic and optical properties of ZnS, ZnSe and ZnTe under pressure", *Computional Material Science*, (38): (2006) 29.

[8] C. W. Jürgen Hafner & G. Ceder, "Toward computational materials design:the impact of density functionaltheory on materials research", *Physical Review C*, **31** (2006).

[9] G. Kresse & D. Joubert, "From ultrasoft pseudopotentials to the projector augmented wave method", *Physical Review B*, **59(3)**: (1999) 1758–1775.

[10] K. Dewhurst & S. Sharma, "Development of the elk lapw code", *Max Planck Institute of Microstructure Physics*, (2011).

[11] W. Kohn & L. J. Sham, "Self-consistent equations including exchange and correlation effects", *Physical Review*, **140**: (1965) A1133-A1138.

[12] Vanderbilt & David, "Soft self-consistent pseudopotentials in a generalized eigenvalue formalism", *Physical Review B*, **41**: (1990) 7892-7895.

[13] J. P. Perdew, K. Burke & M. Ernzerhof, "Generalized gradient approximation made simple", *Physical Review Letters*, **77**: (1996) 3865-3868.

[14] Z. Yingkai & Y. Weitao, "Comment on "generalized gradient approximation made simple"", *Physical Review Letters*, **80**: (1998) 890.

[15] F. Tran & P. Blah, "Accurate band gaps of semiconductors and insulators with a semilocal exchange-correlation potential", *Physical Review Lettered*, **102**: (2009) 226401.

[16] H. Jiang, "Band gaps from the tran-blaha modified becke-johnson approach: A systematic investigation", *Journal of Chemical Physics*, **138**: (2013) 134115.

[17] H. Monkhorst & J. Pack, "Special points for brillouin-zone integrations", *Physical Review B*, **13**: (1976) 5188.

[18] A. Guillermet, "Thermodynamic properties of the generalized murnaghan equation of state of solids", *International Journal of Thermophysics*, **16**(4) (1995).

[19] P. Ravindran, L. Fast, P. A. Korzhavyi, B. Johansson & J. Wills, "Density functional theory for calculation of elastic properties of orthorhombic crystals: Application to tisi2", *Journal of Applied Physics*, **84**: (1998) 4891.

[20] O. M. Landolt-Börnstein New Series, Eds. K.-H. Hellwege, "Numerical Data and Functional Relationships in Science and Technology", volume 22a. Springer-Verlag, 3rd edition, (1982).

[21] R. Franco, P. Mori-Sánchez & J. M. Recio, "Theoretical compressibilities of high-pressure ZnTe polymorphs", *Physical Review B*, **68** (2003).

[22] H. Cheng, Y. C. Li, G. Li, & X. D. Li, "Structural phase transitions of ZnTe under high pressure using experiments and calculations". *Chinese Physics Letters*, **33(9)** (2016).

[23] M. Z. Huang & W. Y. Ching, "Calculation of optical excitations in cubic semiconductors", *Physical Review B*, **47**: (1993) 9446.

[24] R. Gangadharan, V. Jayalakshmi, J. Kalaiselvi, S. Mohan, R. Murugan & B. Palanivel, "Electronic and structural properties of zinc chalcogenides ZnX X = S, Se, Te", *Journal of Alloys and Compounds*, **22** (2003).

[25] C. Soykan, S. Ozdemir & T. Cagin, "Structural and mechanical properties of ZnTe in the zincblende phase", *International Scientific Journal*, **46** (2010).

[26] J. G. Lee, "Computational materials science: An introduction", CRC Press, 2nd edition, (2016).

[27] Heyd, J. E. Peralta, G. E. Scuseria & R. L. Martin, "Energy band gaps and lattice parameters evaluated with the heyd-scuseria-er, zerhof screened hybrid functional", *Journal of Chemical Physics*, **123**: (2005) 174101.

[28] X. Chen, A. Muntz, X. H. J. Hu & J. Zinck, "First principles studies of band offsets at heterojunctions and of surface reconstruction using gaussian dual-space density functional theory", *Journal of Vacince Science and Technology B*, **13**: (1995).

[29] B. H. Lee, "Pressure dependence of the second -order elastic constants of ZnTe and ZnSe", *Journal of Applied Physics*, **41**(7): (1970) 2988-2990.

[30] T. Jia-Jin, J. Guang-Fu, C. Xiang-Rong & G. Qing-Quan, "Phase transition and phonon spectrum of zinc-blende structure ZnX (X = S, Se,Te)", *Commununication Theory Physics*, **53**: (2010) 1160-1166.

[31] W. Martienssen, "Numerical data, volume 22a. Springer handbook of condensed matter and materials data, H. Warlimont (Ed.)", Springer, Berlin, 3rd edition, (2005).

[32] P. Mao, B. Yu, Z. Liu, F. Wang, & Y. Ju, "First-principles investigation on mechanical, electronic, and thermodynamic properties of Mg2Sr under high pressure", *Journal of Applied Physics*, **117**: (2015).